Heliyon 10 (2024) e31419

Contents lists available at ScienceDirect

Heliyon

journal homepage: www.cell.com/heliyon

Research article

Optimal scheduler for energy consumption reduction in multi-vector energy management systems: A case study at the Port of Borg

Joaquim Massana [b,*], Llorenç Burgas [a], Joan Colomer [a], Andreas Sumper [b], Sergio Herraiz [a]

[a] Universitat de Girona, Control Engineering and Intelligent Systems, Campus Montilivi, EPS IV, Girona, 17003, Catalonia, Spain
[b] Universitat Politecnica de Catalunya, Dept. of Electrical Engineering, ETSEIB, Pav. G 23.25, Av. Diagonal 647, Barcelona, 08028, Catalonia, Spain

ARTICLE INFO

Keywords:
Optimal scheduling
Multi-vector energy manager system
Flexibility
Cranes
EV charging station
Microgrid

ABSTRACT

The objective of microgrid operation is to supply the energy demanded by the loads at minimum cost. To achieve this goal, new tools are being proposed in the literature, such as the use of optimal schedulers in the field of multi-vector management systems. An optimal scheduler provides the hourly schedule of the flexible loads that exist in a microgrid to maximize the use of local renewable resources. This work aims to investigate the application in the context of five optimization algorithms in terms of energy and computation costs and to demonstrate how optimal schedulers can contribute significantly to reducing energy operating costs in new and real microgrid scenarios. The analysis of the algorithms is carried out through an experimental process on the existing installations at Port of Borg (Norway), which contains photovoltaic production and different types of flexible assets, such as cranes, electric vehicle charging stations, and electrical storage. Real data gathered at the port's premises is used to assess the energy cost reduction when the optimal scheduler is part of the energy management system, and the computations are performed in real time to apply the proposed schedule to the pilot. The results show how the use of optimal schedulers can reduce operation costs up to 17.2%, augmenting local energy production utilization, and that using two OS algorithms in cascade can also reduce the computation time.

1. Introduction

Nowadays, introducing renewable energy sources into electrical energy systems is reducing reliance on conventional energy resources [1] and the global warming [2]. Main renewable energy sources, such as wind and solar energy, present generation uncertainty due to the variable nature of their primary energy sources. The previous inherent intermittence and uncertainty present difficulties to the daily operation of local energy systems or microgrids. The MVEMS scheduling pursues the minimisation of operational costs in terms of energy or CO_2 emissions [3]. The timing of energy consumption or peak energy demand determines the

* Corresponding author.
E-mail addresses: joaquim.massana@udg.edu (J. Massana), llorenc.burgas@udg.edu (L. Burgas), joan.colomer@udg.edu (J. Colomer), andreas.sumper@upc.edu (A. Sumper), sergio.herraiz@udg.edu (S. Herraiz).

https://doi.org/10.1016/j.heliyon.2024.e31419
Received 14 February 2024; Received in revised form 14 May 2024; Accepted 15 May 2024

Available online 21 May 2024

Acronyms

BESS	Battery electric storage Systems	MG	Microgrids
CHP	Combined heat and power	MT	Micro turbine
DE	Differential evolution	MVEMS	Multi-vector energy management system
EF	Energy forecaster	MVPA	Most valuable player algorithm
EV	Electric vehicle	NRL	Non-responsive loads
GA	Genetic algorithm	OS	Optimal scheduler
GSA	Gravitational search algorithm	PEM	Proton-exchange membrane
HVAC	Heating, ventilation, and air-conditioning	PSO	Particle swarm optimization
HB-ACO	Bacterial foraging ant colony optimisation	PV	Photovoltaic
HT	Hydrogen tank	PWT	Potable water tank
IMOBA	Improved multi-objective bat algorithm	RLD	Responsive loads
LES	Local energy systems	ROD	Reverse osmosis desalination
LFCARO	Levy flight and chaos-assisted artificial rabbits optimisation	RTG	Rubber-tired gantry
		SA	Simulated annealing
LM	Lagrange multipliers	SOC	State of charge
LS	Least squares	WT	Wind turbines

price dynamics of energy in the market. Moreover, optimal scheduling requires forecasting of non-controllable demand and generation. Developing an OS module within the MVEMS will help solve these challenges. OS objectives should prioritize optimizing local renewable generation usage, enhancing system autonomy, and reducing overall energy expenses, peak loads, and CO_2 emissions, among additional optimization criteria. [4].

The optimisation of an MVEMS must be performed by scheduling the operation of controllable assets, i.e., flexible assets, such as EV chargers, BESS, thermal systems, or diesel generators. The management of these assets have to be done collectively, and decisions on when to consume, produce, or store electric energy must be made. The objective is to provide a schedule for these assets' operations. This scheduling plan is based on forecasting non-controllable local energy production and consumption. Then, during the optimal scheduling process, controllable installations must be modelled to simulate their energy consumption. Finally, an optimisation solver must solve a problem with an objective that is defined from a mathematical functions mix, including existing technical and operational requirements and constraints of the assets.

The following text addresses the state-of-the-art optimal schedulers for Energy Consumption Reduction in Multi-Vector scenarios. In the past years, different OS working over MVEMS have been proposed in the literature [3,5,6,19]. In [3], an overview of state-of-the-art MVEMS is presented, where a table gathers which assets are managed by the EMS (flexible assets), non-controllable consumption assets (non-flexible demand), non-dispatchable generation installations, existing demand, and generation. The referenced table also incorporates information on the application of real data and the nature of the tests conducted in actual installations. Lastly, it provides details on the solver and the algorithm used to compute an optimal scheduling plan for the controllable assets.

From the assets' point of view, all the works include battery BESS [7–20], and only some of them include other controllable assets such as MT [7,8,11,13,16,18,19] or RLD [7], HT [7,10], PWT [10], ROD [10] or CHP [15,18]. According to the non-controllable assets, almost all works contain PV modules PV, WT, or both. There are NRL [7,9–11,13,15] in more than half of the works, and there is one work [10] where a non-controllable load is defined as a PEM fuel cell.

From the optimisation point of view, a large number of solvers have been tried. There are solvers that use linear programming [12,13], LM [14], non-linear programming [9], and multi-agent systems [10], but the rest use stochastic methods such as MVPA [15], HB-ACO [17], LFCARO [20], IMOBA [16] or GSA [7]. There is only one work [9] wherein actual weather data is used to build the models. The rest of the publications do not include actual data or implementation and are based on theoretical scenarios. Moreover, most reviewed works do not consider the computational time needed to conduct the optimisation processes. These works use methods that are hard to use in real time because their huge computational requirements, such as calculation time and latency. To the best of our knowledge, there are no use cases or pilots in which assets such as cranes are scheduled, nor works in which these assets are scheduled testing several heuristic methodologies on real scenarios. Finally, in a general manner, the experimental scenarios are small.

In summary, the main drawbacks of the tools proposed in the literature are: a) mainly synthetic data, not real data gathered in the field, is used to model the assets; b) they do not include information about computational cost, which is needed to compare or assess their implementation in a real environment; c) flexible assets as electric cranes are not considered; d) just few algorithms are tested; and e) they are not designed to be implemented in a real scenario but to perform off-line experiments. All this information is summarised in Table 1.

In the previous work, the authors [3] proposed a real case of an OS to perform a 24-hour day-ahead schedule over present controllable installations, including EV charging stations, an HVAC system, a hydrogen refuelling station, and an electrolyser. The OS regulates the HVAC system with a focus on optimizing energy usage and capitalizing on economic incentives. This entails adjusting electricity consumption to off-peak hours, resulting in decreased electricity expenditures. The shifting of the load, additionally,

Table 1
Advantages of the current work.

	Multiple solvers tested	Cranes inclusion	Real data used	Computer Cost comparison	Real implementation
NO	[7,9–14,16,17,19]	[7–20]	[7–20]	[7–20]	[7–20]
YES	[8,15,18,20] [Current work]	[Current work]	[9] [Current work]	[Current work]	[Current work]

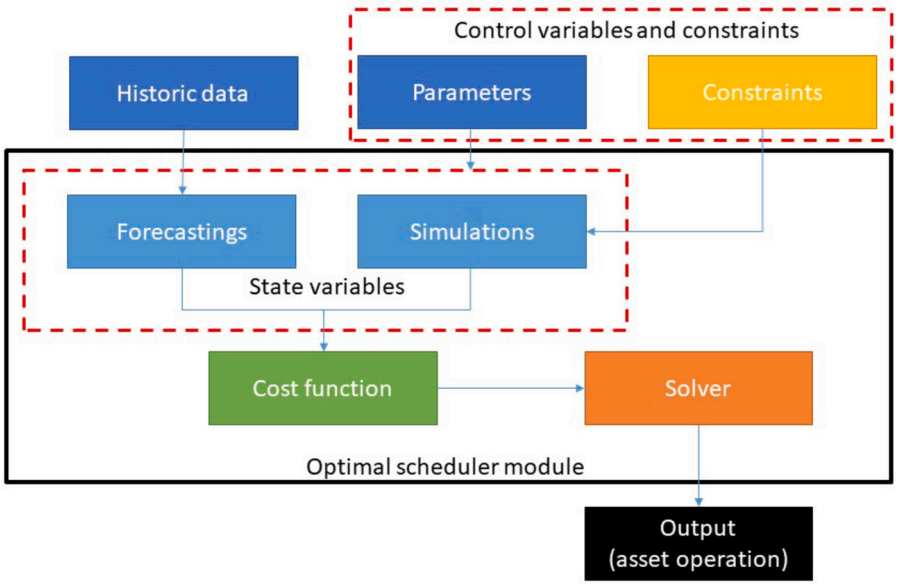

Fig. 1. System diagram of the OS, that is outputs and inputs, and the internal parts.

applies to EV charging stations and the electrolyser, promoting the utilization of green mobility and diminishing CO_2 emissions while the utilization of local generation resources increases.

To overcome the limitations of the previous works, this paper presents a novel use case and real validation case of optimisation of a hybrid MG situated in a port in Norway with multiple controllable assets and distinct energy sources. In this case, a PV unit is the local renewable source, while controllable assets comprise two RTG cranes, eight EV chargers, and a BESS. In addition, there is a thermal asset, but in this case, this is solved using a classical control. Also, a set of distinct solvers, such as GA [21], PSO [22], etc., have been tested and evaluated. The solvers are compared in terms of computation time and the accuracy of the obtained solution. Moreover, the robustness of the proposed methodology is analysed by comparing the optimal solution found, based on forecasted data, concerning the real solution, based on real data, and the result of applying a non-optimised schedule.

The paper is structured as follows. Section 2 presents the general methodology followed to implement the OS. Next, Section 3 describes the case study to test the OS. Section 4 shows the results obtained in the tests, compares different solvers, examines the robustness of the solutions against inaccuracies in the input data, and analyzes the best results provided by the OS. Finally, Section 5 presents the conclusions of the work.

2. General methodology

This section describes the OS module based on the description of the above-mentioned MVEMS. The OS is software that is part of the MVEMS and computes the hourly day-ahead schedule of the controlled assets in the energy grid to reach the stated goal.

Fig. 1 summarizes the complete landscape of the OS module. OS module is divided into several internal parts, inputs and output. As Fig. 1 shows, inputs can be placed in the following groups, historical data, parameters and constraints.

- Historic data (dark blue box): Data from prior states of the non-controllable assets.
- Parameters (dark blue box): Configuration of the simulated assets.
- Constraints (yellow box): User-defined or technical constraints on the assets.

In Fig. 1 can be seen that internal OS parts are the solver, cost function and state variables.

- Solver (orange box): The algorithm used to solve the optimization problem.

- Cost Function (green box): The objective function to be optimized and composed of state variables.
- State Variables (red dotted box): the inputs of the cost function are called state variables and can be divided into forecasting and simulations.
  - Forecastings (blue box): Assets that can not be controlled. These models require as input historical data (Dark blue box).
  - Simulations (blue box): Controlled Assets. These models require Parameters (Dark blue box) and can be affected by constraints.

Output (black box) of the OS module is the operation of the controllable assets for the next day.
The next subsections will focus on state variables, control variables and constraints, and cost function and solver.

2.1. State variables

The inputs of the cost function are called state variables. The state variables mathematically contribute to defining the objective to be optimised. For the cases of generation and consumption, there are different types of state variables depending on the asset. State variables can be energy values, such as electrical or thermal energy consumption, PV generation, or EV charging stations.

Energy demand is calculated using different approaches depending on whether the demand is controlled or non-controlled. In the first case, the OS module simulates the energy consumption because it relies on the controlled operational state of the asset. Various methodologies, such as equation models, are tested to simulate the controllable assets. In the second case, an EF, based on historical consumption or generation data, weather forecasts (temperature, global radiance, etc.) and other contextual information (day type and day hour), predicts the energy generation or usage.

2.2. Control variables and constraints

The parameters that can be changed to operate the assets in a certain way are called control variables. Those variables' value is the OS's output to reach an optimal operation of the system. An example of a control variable is the maximum discharge power of an electric battery or the number of movements to be made for each time slot on the port cranes.

The constraints represent the limitations on the assets, both technical and operational. They can be continuous or discrete and defined by a maximum, a minimum, or a range. An example of a constraint is the maximum capacity of an electric battery.

2.3. Cost function and solver

The objective pursued by the OS when calculating the schedule of the controllable assets is described by the cost function. The cost function considers the state variables, the control variables, and the constraints, including the cost of the energy supplied by the distribution power system. To find the best combination for the control variables, that is, the set of values that minimize the cost function and maximize the desired goal, the OS uses a solver algorithm.

3. Description of the case study

The present section describes the asset optimisation done by the MVEMS in a pilot located in the Port of Borg. The Port of Borg is placed in an industrial area on a small peninsula called Øra, just outside Fredrikstad, Norway. The harbour moves approximately 3,400,000 tons of goods annually for private and public customers. The pilot contains the following energy domains: electrical energy, electrical storage, electricity-to-thermal and electricity-to-movement. The different energy usages are identified in Fig. 2, according to each bus seen in the legend. In Fig. 2, the assets present in the MG are also shown. There are three types of assets: consumption (sink), power supply (source), and storage.

The local energy generation unit and the electric grid supply the electricity required for the installation. The local energy generation unit comprises a PV plant of 2,000 kWp. Concerning demand, on the one hand, the controllable demand in the harbour is composed of two RTG cranes, eight EV chargers of 7.2 kW each, one BESS, and the thermal system, which also consumes a slight electrical power. The first set of assets is scheduled by the OS, while the thermal system is controlled independently based on rules due to the available data and the features of this installation. On the other hand, the non-controllable demand in the harbour consists of other electrical loads, mainly buildings, harbour lights, and non-controllable cranes.

To enhance the MG operation, optimise the use of local renewable resources, and minimising the operational costs, the EMS manages the following controllable variables: the number of movements performed by the cranes along the day, the stored energy in the batteries and the energy provided by the EV chargers to cars.

3.1. Implementation of the case study

The OS for the Port of Borg MG is applied, concreting the needed inputs (state variables), the outputs (control variables), and the technical and operational constraints, and finally the cost function. Fig. 3 provides a wide description of the OS design.

3.1.1. State variables

The state variables are necessary to define the cost function and provide information on the cost of using a particular solution. Two types of variables can be found according to their origin: the forecast and the simulated variables. The predicted variables are

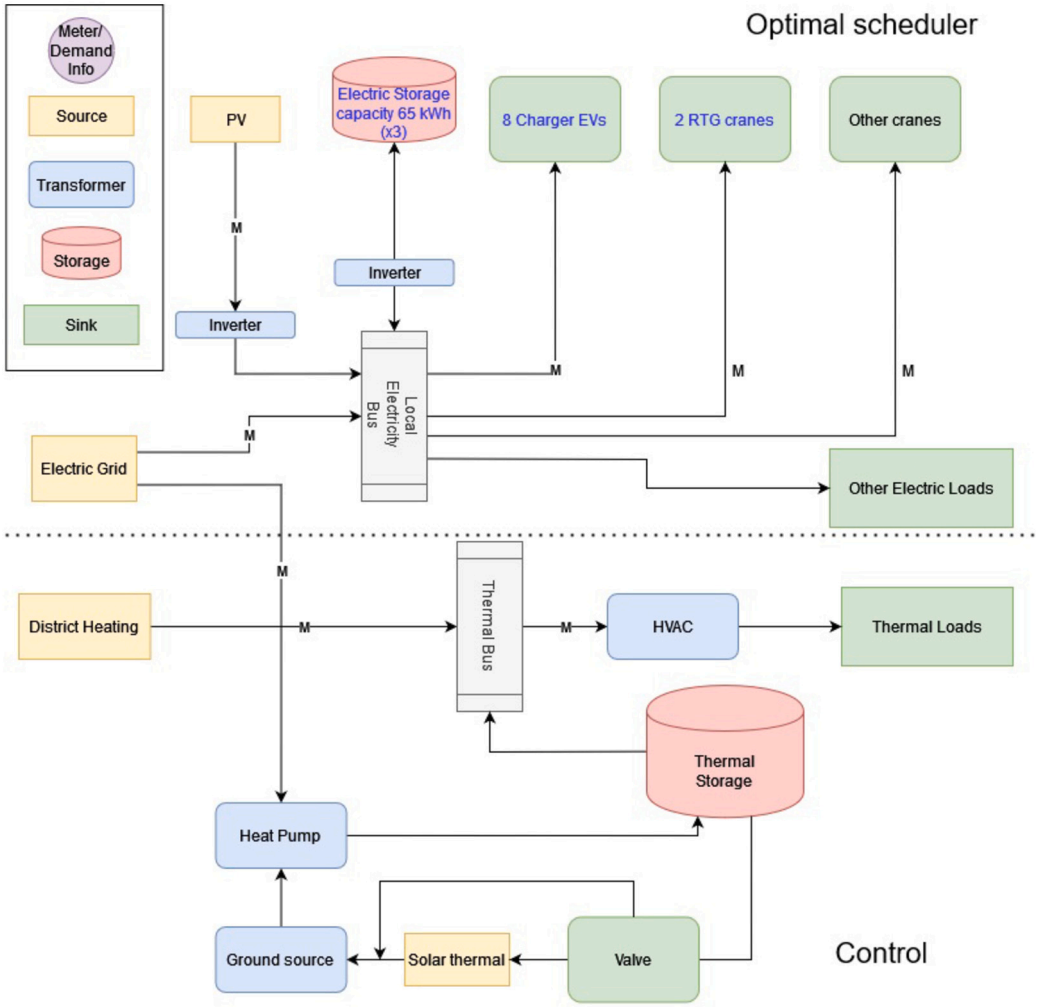

Fig. 2. Port of Borg installations and assets. The controllable assets are in blue letters.

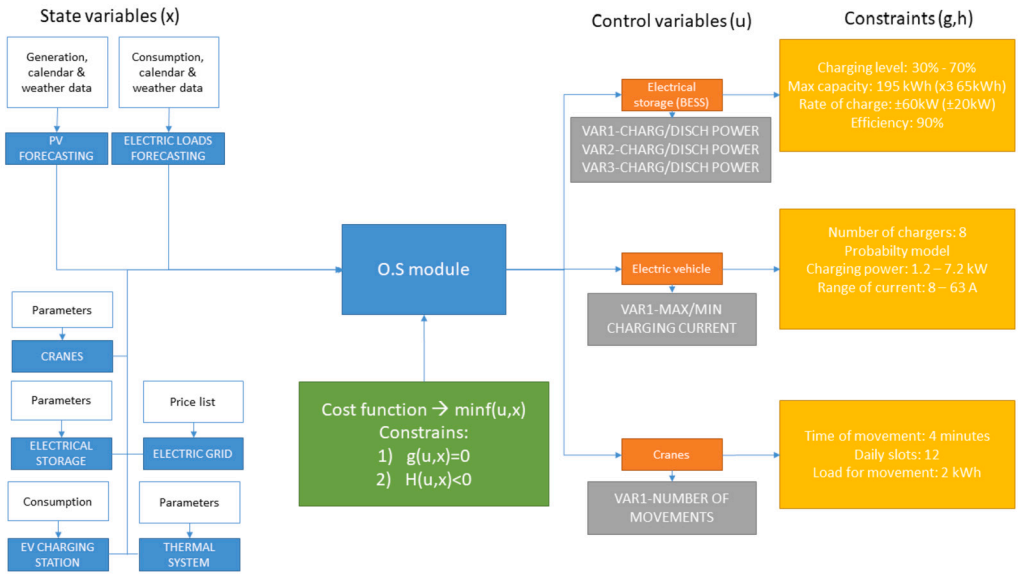

Fig. 3. Port of Borg pilot: block diagram of the OS.

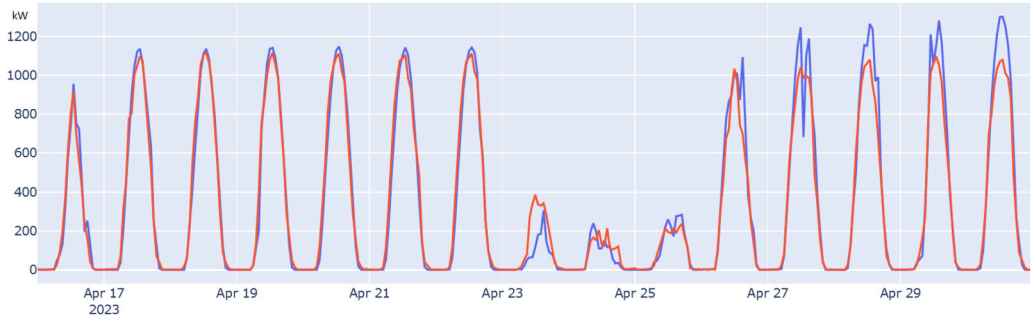

Fig. 4. PV generation forecasting. The x-axis is the time in hours, and the y-axis is the energy generated in kW. In blue is the real electrical generation, and in red is the prediction performed by the model.

Table 2
Performance statistics of PV generation forecasting.

MAE (kW)	R^2	CC	MAPE
42.844	0.967	0.985	1.423

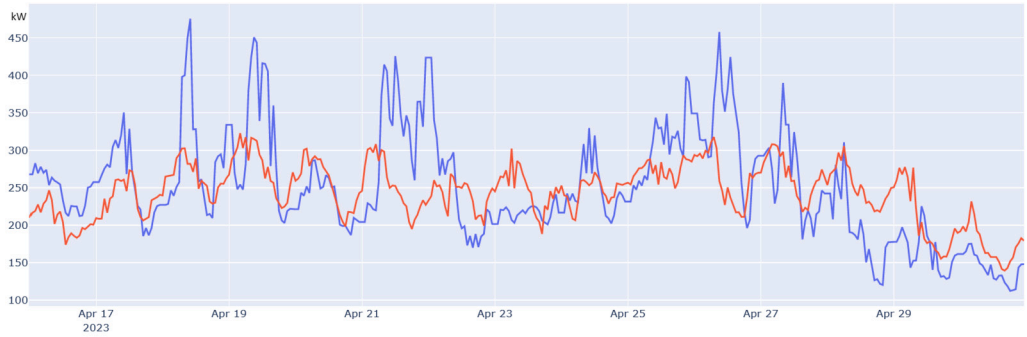

Fig. 5. Non-controllable consumption forecasting. The x-axis is the time in hours, and the y-axis is the energy consumption in kW. In blue is the real electrical load consumption, and in red is the prediction performed by the model.

Table 3
Table of performance statistics.

MAE (kW)	R^2	CC	MAPE
47.722	0.298	0.555	0.191

computed using machine learning models, and the simulated variables are computed using equations. Next, the state variables in the case study are described.

- **PV generation:** For forecasting the electric energy produced daily (D_{GEN}) in the PV plant, a histogram-based gradient boosting regression tree model [23] is used. Here, as not much technical data was provided, a statistical modelling technique is applied. Bottom-up techniques such as the ones used in [24] require much technical data not available here. The model is generated using historical records of data of PV generation and weather. Data was scaled using standard escalation, that is, to standardize features by removing the mean and scaling to unit variance. All observations with missing values were deleted. As an example, Fig. 4 presents the real generation in the PV and the predicted generation in the PV for the best model configuration found; see Table 2 with the performance statistics (mean absolute error, R-squared, coefficient of correlation, and mean absolute percentage error) corresponding with the best set of parameters (maximum bins 86, maximum depth tree 15, and minimum samples per leaf 5).
- **Non-controllable consumption:** daily electrical consumption (D_{NCON}) for the assets that the OS does not directly schedule is computed with a forecasting model created using a histogram-based gradient boosting regression tree model [23]. Data was scaled using standard escalation, and all registers with empty data were deleted. As an instance, Fig. 5 depicts the actual consumption and the prediction of consumption for the data of test for the best model configuration found; see Table 3 with the performance statistics corresponding with the best set of parameters (maximum bins 200, maximum depth tree 14, and minimum samples per leaf 3).

This prediction presented difficulties in performing, and thousands of models were trained to achieve this middle-low level of performance in the prediction. These difficulties were due to the nature of the data set, which includes a high level of variability in the consumption patterns. Also, consumption processes depend on non-available information (i.e., non-controllable crane movements depend on the ship arrivals, and this data is not available for calculations). In addition, the data set includes noise and inconsistencies. This kind of difficulty can be found when applying such technical solutions in real scenarios.

- **Electric vehicle charging stations:** energy that consumes the EV charging station (D_{EC}) is computed using a probabilistic model of how cars arrive at the charging station and the features of the installation itself, as shown in Eq. (1). Concerning the probability of having a car plugged on one charge, the EV charging sessions of the Port of Borg pilot have been clustered among generic user profiles following the methodology exposed in [25] and using bi-variate Gaussian mixture models as a clustering method. Eight user profiles have been found for this case study, each with its Gaussian model in terms of connection starting time and connection time. At the same time, every user profile has an average weight over the average number of sessions per day. These features have been used to simulate charging sessions for a whole year, obtaining the corresponding occupancy profiles and calculating the occupancy probability considering the pilot's eight charging stations.

$$D_{EC} = \sum_{i=1}^{24} [Charging\ power(i) \cdot NoC \cdot Prob \cdot \Delta t] \in (2.3, 25) \tag{1}$$

where:
D_{EC} = daily energy consumed by EV charging stations (kWh).
NoC = number of chargers (8 in this case).
$Prob$ = probability of having a car charging on one charger.
$Charging\ power$ = power that chargers can charge (from 0 to 7.2 kW).
Δt = time increment (1 hour).

- **Electricity price:** day-ahead hourly electricity prices (D_{EP}) are gathered from external providers [26].
- **Controllable cranes:** day-ahead hourly electricity consumed by controllable cranes (D_{CRANE}) is computed starting from the number of movements performed by the cranes and the energy consumed in each movement, as seen on Eq. (2).

$$D_{CRANE} = \sum_{i=1}^{24} [Energy\ of\ movement \cdot Number\ of\ movements] \tag{2}$$

where:
D_{CRANE} = total energy consumed by controllable cranes (kWh).
$Energy\ of\ movement$ = constant and equal to 2 kWh.
$Number\ of\ movements$ = number of movements in 1 hour.

- **Electrical storage:** This input is used to simulate the SOC of the battery, calculating the energy consumed in the process of charging and the energy provided by the battery when discharging, and knowing the SOC at a particular moment. Equations (3) and (4) reproduce the behaviour of the battery:

$$D_{ES} = \sum_{i=1}^{24} [Power(i) \cdot \Delta t] \tag{3}$$

where:
D_{ES} = total energy consumed/generated by the battery during one day (kWh).
$Power$ = charging/discharging power in which the battery is charged/discharged for 1 hour (kW).
Δt = time increment (1 hour).

$$SoC(i) = SoC(i-1) + (Energy_C(i) \cdot Efficiency) - Energy_P(i) \tag{4}$$

where:
SoC = state of charge, that is the quantity of energy that is stored in the battery (kWh).
$Energy_C$ = energy used to charge the battery (kWh).
$Energy_P$ = energy delivered by the battery (kWh).
$Efficiency$ = efficiency of the battery.

- **Thermal system:** The electrical heat pump is turned on and off depending on the solar contribution to the system. Suppose the thermal system has enough solar contribution. In that case, the electrical consumption will be 3 kW, whereas when there is no solar contribution, the consumption will be zero, as this asset is turned off. It is worth mentioning that all the thermal energy requirements not fulfilled for this asset are acquired from a district heating.
  A study based on historical data of thermal production and solar radiance showed that the thermal solar panels could produce enough heat to put the asset in on mode following the rules in Table 4, whereas the hours when the condition on global radiance is not satisfied or out of the table, the asset will be set at off mode.

Table 4
Conditions on solar thermal asset position (ON mode) when global radiance (W/m^2) exceeds the value on the table.

3 h - 6 h	7 h	8 h	9 h-16 h	17 h	18 h	19 h - 21 h
> 400	> 300	> 250	> 200	> 250	> 300	> 400

Equation (5) and Table 4 reproduce the behaviour of the thermal assets:

$$D_{Th} = \sum_{i=1}^{24} [Power(i) \cdot \Delta t] \tag{5}$$

where:
D_{Th} = daily energy consumed by the thermal asset (kWh).
$Power$ = power consumed by the asset according to its mode (kW).
Δt = time increment (1 hour).

3.1.2. Control variables and constraints

Controllable assets in Port of Borg can be seen in Fig. 1. These assets are EV chargers, cranes, and BESS, and the parameters and constraints related to each controllable asset are explained in this subsection.

EV charging station: OS schedules the power that the EV chargers can provide to the cars. As commented above, the pilot has 8 chargers, being the total supplied electric power, the variable that can be controlled. Moreover, the OS has to respect the subsequent specifications and technical requirements:

- The minimum charging power set-point per charger equals 0 kW.
- The maximum charging power set-point per charger equals 7.2 kW.
- The minimum total charging power equals 2.3 kW.
- The maximum total power equals 25 kW.
- There are no time restrictions on the charging process.

Cranes: OS provides the hourly schedule of the container movements of the two RGT cranes, that is, how many movements should be made at each time slot. The number of crane movements depends on the planned ship arrivals, which can not be postponed. This number of movements is received daily by email. Besides, the OS has to meet the subsequent specifications and technical requirements:

- Each crane movement takes 4 minutes.
- Each crane movement consumes 2 kWh.
- There are 2 controllable cranes.
- Cranes can only be operated from 6:00h to 18:00h.
- All the movements must be done during the current day.

BESS: The OS schedules the hourly charging or discharging power for each of the three existing batteries. Besides, the OS has to meet the subsequent specifications and technical requirements:

- Each battery has a capacity of 65 kWh.
- The maximum charge rate equals 20 kW.
- The maximum discharge charge rate equals 20 kW.
- Minimum SOC level equals 30%.
- Maximum SOC level equals 70%.
- The charge of a battery has an efficiency of 90%.
- There are no time restrictions for charging/discharging the battery.

3.1.3. Cost function

The cost function (aka objective function) is what the OS aims to minimise. The cost function is defined as a day-ahead operational cost approximation. By doing so, the OS will find the most effective combination for the control variables to minimize the operational cost of the day-ahead. In this way, defining the cost function as an operational cost will integrate the maximum self-consumption of local generation as possible to the MG.

In the cost function, the three controllable assets are defined. In addition, function cost includes the electricity price given by the utility. This energy is the energy consumption (buildings, lights, cranes, EV charging stations and electrical storage) and local generation (PV and BESS) difference.

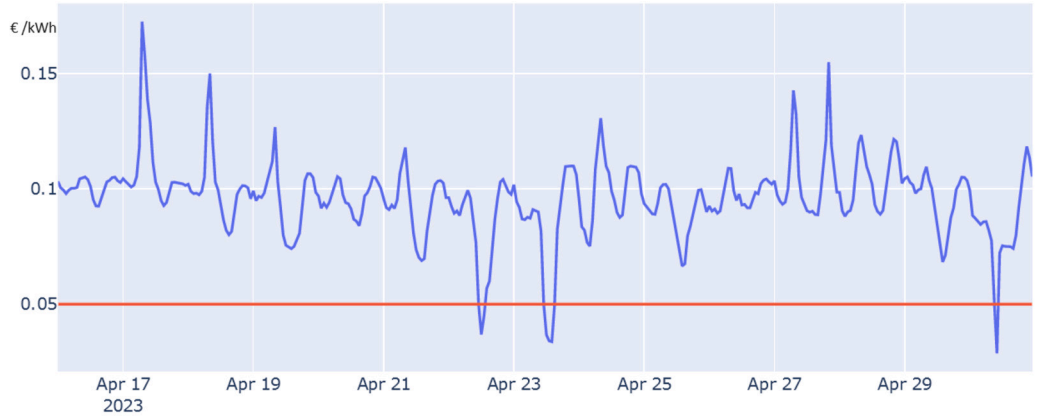

Fig. 6. Energy prices are introduced in the simulations. The x-axis is time in hours, and the y-axis is energy price in euros/kWh. The blue line is the energy buying price, and the red line is the energy selling price.

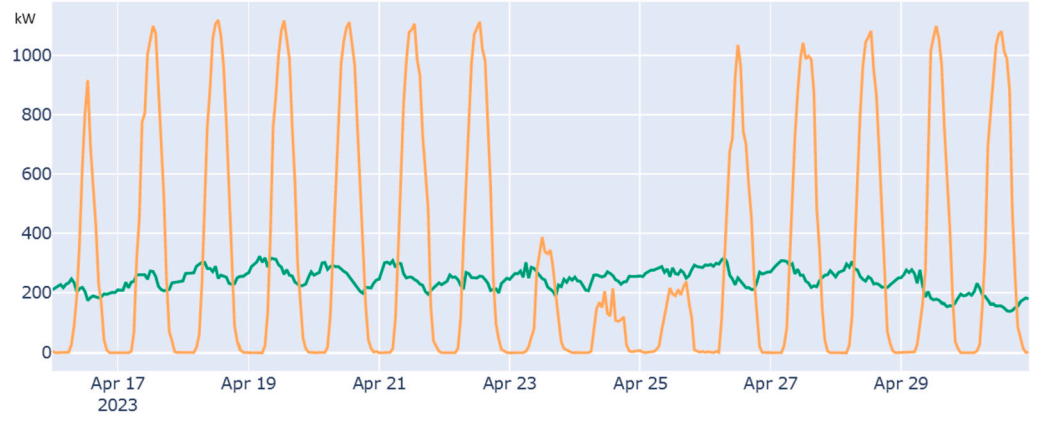

Fig. 7. Forecasted energy consumption and generation are introduced in the simulation. The x-axis is time in hours, and the y-axis is in kWh. The orange line represents PV generation, and the green line represents non-controllable demand and thermal consumption.

The cost function is shown in Equation (6):

$$f(control\ variables) = P_e \cdot [D_{NCON} + D_{CRANE} + D_{ES} + D_{EC} + D_{Th} - D_{GEN}] \tag{6}$$

where:
D_{NCON} = aily electrical energy consumption in all the non-controllable assets (kWh).
D_{CRANE} = daily electrical energy consumed by the cranes (kWh).
D_{ES} = total energy consumed (positive)/provided (negative) by the battery during one day (kWh).
D_{EC} = daily electrical energy consumed in the EV chargers (kWh).
D_{GEN} = daily electrical energy generated in the local generation resources (kWh).
D_{Th} = daily electrical energy consumed in the thermal asset (kWh).
P_e = energy prices: the price of the energy sold to the grid is fixed at 0.05 euros/kWh, but it is dynamic for buying energy.

4. Results and discussion

This section shows an example of the proposed OS application in Section 2 to the MG depicted in Section 3. As can be seen in Section 3, the generation and consumption of non-controllable assets is forecasted while the consumption of controllable ones is modelled using equations. The objective of the optimization is minimizing the operation cost, which is expressed in the cost function shown in Equation (6). This example corresponds to the optimisation of the MG for 15 days, using a data set from the 16^{th} to the 30^{th} of April 2023. During this period, each day at 23:55, the data is collected from the MG by several web services through a middleware platform to calculate the optimal hourly schedule of controllable assets for the next day.

First of all, the variables that influence the OS results are displayed in Figs. 6 and 7. Fig. 6 shows the hourly electricity buying and selling prices, and Fig. 7 displays both forecasted energy generation and consumption of non-controllable assets. The initial SOC of the batteries and the planned number of crane movements to be made each day are shown in Table 5.

Table 5
Prevision on crane movements and initial real battery SoC.

day	Cranes	SoC
Apr 16	0	58.5
Apr 17	30	58.5
Apr 18	70	58.5
Apr 19	250	58.5
Apr 20	0	58.5
Apr 21	450	58.5
Apr 22	70	58.5
Apr 23	0	58.5
Apr 24	0	58.5
Apr 25	200	58.5
Apr 26	130	58.5
Apr 27	50	58.5
Apr 28	0	58.5
Apr 29	0	58.5
Apr 30	0	58.5

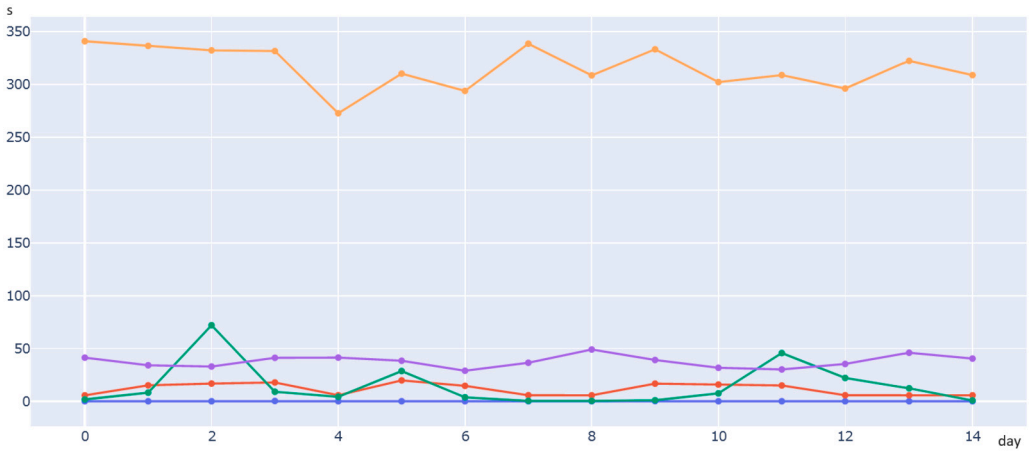

Fig. 8. Computing time in seconds for each day and for each solver. The y-axis is the time in seconds, and the x-axis is the day of the simulation. The blue line is LS, the red line is SA, the green line is DE, the purple line is PSO, and the orange line is GA.

With the information shown in the Figs. 6, 7, and Table 5, the OS provides an hourly optimal plan for the day-ahead operation of controllable assets.

4.1. Results

Once the energy consumption and generation forecasts of non-controllable assets are calculated and available to the OS, together with the predefined requirements and technical specifications of the assets and energy prices, the cost function, Equation (6), is solved. The goal of the solver is to find the best combination of the control variables for minimizing the value of the cost function.

A set of distinct solvers has been tested to evaluate their performance in terms of computation time and the goodness of the solution that they provide. Next, a study on the effect of forecast errors on the OS solution is performed. Finally, an analysis of the best results obtained is presented.

4.1.1. Solver comparison

The present cost function is defined by using a mix of techniques; some of them are based on mathematical formulations, while others are based on statistical models. Usually, meta-heuristic techniques are applied with this kind of cost function.

In the application example, five distinct solvers have been tested to assess the solution's quality and the required computing time in an Intel i7-9800X with 64 GB of RAM. The selected solvers are GA [21], PSO [22], SA [27], DE [28], and LS [29]. SA, DE, GA, and PSO are the heuristic branch's most common classical or commonly used optimization techniques, whereas LS is a non-heuristic technique. Despite the type of the present cost function, LS is also tested, but it is not capable of finding solutions on all the tested days, as this solver makes assumptions on the cost function that are not always met in the current problem.

First of all, Fig. 8 shows a comparison of the computing time needed to calculate each daily schedule with each solver.

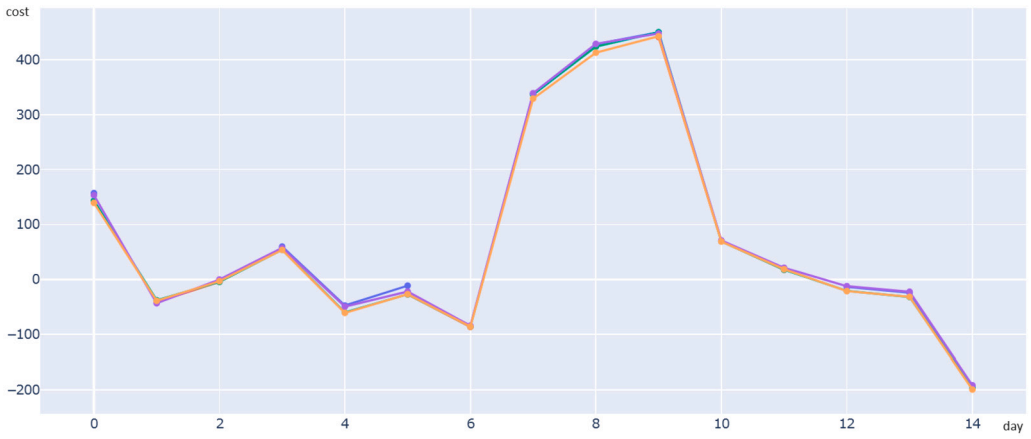

Fig. 9. Operation cost for each day and each solver. The y-axis is the simulated cost in euros, and the x-axis is the day of the simulation. The blue line is LS, the red line is SA, the green line is DE, the purple line is PSO, and the orange line is GA.

Table 6
Cost in euros achieved for the best solution found by each solver in a real and simulated scenario for 14 days. Change between both scenarios (real data, simulated data).

	LS	SA	DE	PSO	GA	Classic Control
Simulated	1452.83	1244.68	1191.01	1288.06	1141.69	– – –
Real	1503.44	1298.72	1240.67	1343.24	1189.54	1436.59
Change %	3.48%	4.34%	4.16%	4.28%	4.19%	– – –

On the other hand, in Fig. 9, a comparison of the best solution cost achieved on each solver can be found. Note that these costs are computed internally by the solver, using the forecasted values of the distinct assets, not the real costs of applying the solution in the pilot the next day.

As can be seen in Fig. 8, GA is the solver that consumes the most computing time (around 300 s) and LS is the least time-consuming one (milliseconds). Although GA needs much more time to calculate the solution, Fig. 9 shows that GA finds slightly better solutions than the other solvers. Regarding the computation time/results ratio, the best-balanced algorithm is DE. Finally, LS does not find always the best solutions but achieves suitable solutions with extremely low computing time in 10 of the 14 days.

In this case, the results show that the best procedure is to find a solution first with LS and, if it is found, use it as a seed in a DE or GA algorithm to speed up the convergence time.

4.1.2. Robustness to forecast and modelling errors

As noted in previous sections, forecasting models cannot predict real energy generation and consumption perfectly, existing a discrepancy between what is predicted and what finally occurs in real-time. So, simulated costs will be slightly affected when computed using the real PV production and controllable and non-controllable assets demand. Also, a classical online control strategy is added to the comparison since this control does not operate over any forecasting, but it performs a logical baseline operation on the assets according to on-time available readings (i.e. the battery is charged if there is a surplus of solar generation and discharged when there is not enough solar generation to cover the electrical consumption). Table 6 shows the costs of operating the assets over real and simulated variables for the whole 14-day period for each solver, as well as the change % between both results. This decrease in performance can be directly attributed to accumulated modelling and forecasting errors; not all the techniques have the same performance decrease because of randomness in parts of the algorithms themselves, as well as the robustness of each methodology against noise changes. Note that LS can only find solutions on 10 out of 14 days. So, in the 4 days without a solution, a completely random operation of the assets was performed, causing a drastic increase in the operation costs.

Although the forecasted data used as input to the OS is not always as accurate as desired, all the OS can achieve better performances than logical online control over the assets. This improvement is because OS considers a global daily vision of the optimization problem.

4.2. Best results analysis

In this subsection, the operation of the assets scheduled by the solver is analysed. The analysed results correspond to the best solution found and applied to the real pilot. According to Table 6, the real cost of the best solution using a day ahead optimal scheduler with GA, compared with a classical control technique based on the leverage of energy surpluses, presented a reduction of 17.2%. As commented, the solution is an hourly day-ahead schedule of the available control variables. This solution is achieved

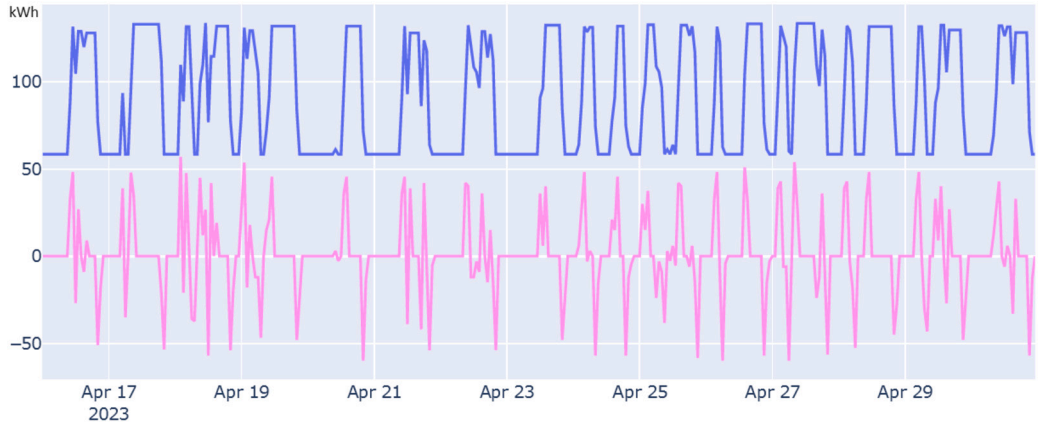

Fig. 10. BESS operation. The x-axis is time in hours, and the y-axis is energy in kWh. The blue line is the SOC of the batteries, and the pink line is the charged/discharged energy.

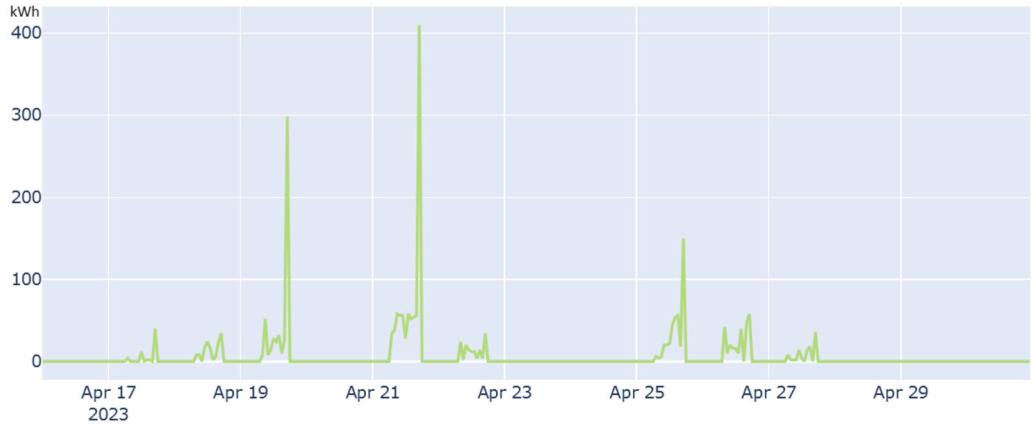

Fig. 11. Cranes operation. The x-axis is time in hours, and the y-axis is the consumed energy by controllable cranes in kWh. The green line is the energy consumed to make the movements planned in each hour.

by the OS with simulations of the controllable assets and forecasting of consumption and generations. Next, the results for each controllable asset are commented on.

BESS is operated by setting the charging or discharging power during each hour. In Fig. 10, the operation of the batteries and the simulated SOC are displayed to understand better how the batteries behave according to the solution provided by OS.

According to the cranes, OS receives by email the number of container movements expected for each day. Then, the OS distributes the movements during the day at the available working hours. In Fig. 11, the consumed energy by the cranes due to the movements of containers planned by the OS for each hour is displayed.

Concerning the EV charging station, the profile on the ampacity of the distribution line that feeds the 8 chargers and the expected consumed energy by all the chargers, according to the simulated occupation of the chargers, is displayed in Fig. 12.

Finally, in Fig. 13, the PV production and the consumption of the assets are displayed, giving an overall view of the performance of the installation. Having a global view of all the assets, the optimizer can operate accordingly to each situation, as can be observed from the Figures. For example, the battery is mainly charged during energy surplus hours and discharged to avoid consuming power from the grid. But some days, the battery is charged and discharged during night hours to exploit energy price variations. Very similar behaviours can be found in the EV chargers and the cranes' consumption that are placed during solar production hours.

5. Conclusions

With the present need to reduce CO_2 emissions, several actors have been proposing new tools. Multi-vector energy management systems improve the performance of the microgrid assets while reducing ambient contamination. These new tools manage several microgrid installations using an optimal scheduler and following diverse optimization criteria. So, this goal is achieved by reducing energy used in the operation of the microgrid through the calculation of an optimal schedule for the flexible assets in the system.

In the present work, several optimal scheduler algorithms, such as genetic algorithm, particle swarm optimization, simulated annealing, differential evolution and least squares, were tested to assess the computation time and the energy operation costs resulting from the execution of the dispatched optimal schedule. According to the obtained results, the fastest technique was least squares,

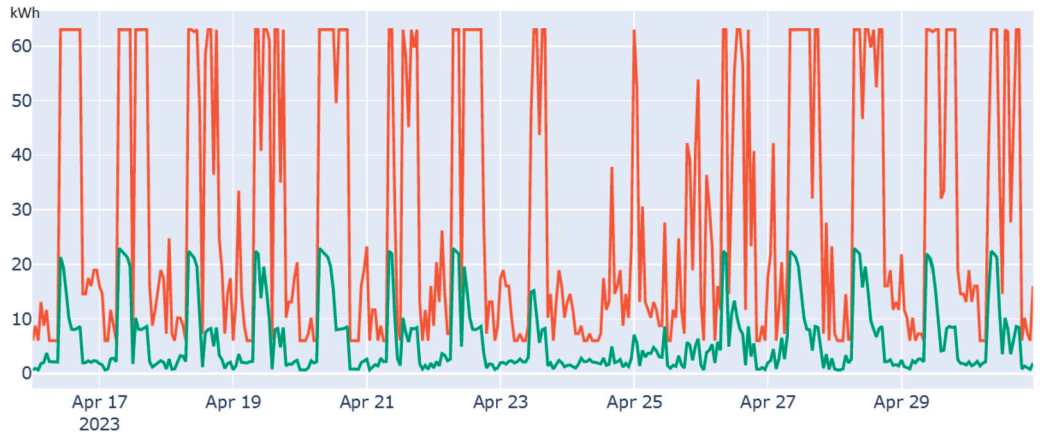

Fig. 12. EV charger operation. The x-axis is time in hours. The green line is the energy consumed by the 8 chargers in kWh. The red line is the total permitted ampacity in Amps.

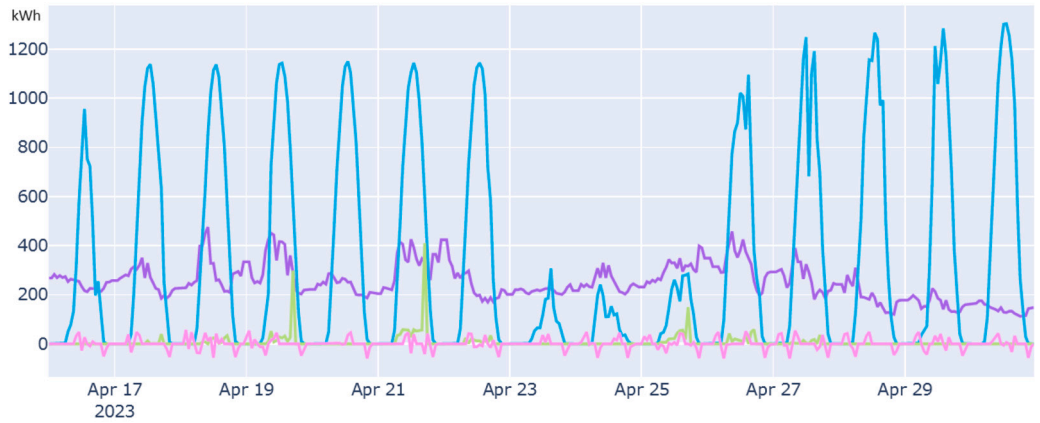

Fig. 13. General operation of the system. The x-axis is the time in hours. The green line is the energy of the cranes in kWh. The pink line is the battery energy in kWh. The blue line is the real solar production in kWh. The purple line is the non-controllable loads in kWh.

some milliseconds, but it does not always find solutions due to the cost function nature. The most time-consuming method was genetic algorithms, around 300 s, but on the other hand, it was also the one providing the best results. The most balanced technique in performance/computing time was differential evolution, around 25 s on average. A combination of algorithms can help to reduce computation costs, achieving better results.

The results produced a considerable reduction in the pilot's operation costs despite the inaccuracies in the forecast calculations. The real energy cost of the system, taking advantage of controlling flexible assets, electricity prices, and using a day ahead optimal scheduler technique, compared with a classical control technique, which is based on energy surpluses when they are produced, presented a reduction of 17.2% with genetic algorithms, 13.6% with differential evolution, 9.6% with simulated annealing, 6.5% with particle swam optimization, and similar with LS. For this last technique, energy cost reduction was only achieved for part of the testing period since the least squares method does not always provide a solution. This fact shows that these optimization tools can be deployed in real systems. The authors demonstrate that although the initial data used to calculate optimal schedules (forecasts) differs from the real data used during the operation, a reduction in terms of cost or energy consumed from the grid can be achieved.

In summary, the proposed solution in this paper can be integrated into an energy management system and put into operation in big real scenarios, with different types of flexible assets, such as a port, reducing considerably the operational costs of the system.

6. Future work

The authors will continue working on the present methodology in future works by testing it in a new pilot at the Valahia University of Târgoviște (Romania). Also, the testing of new assets and aspects such as:

- A comparison between expert knowledge scheduling and OS scheduling will be made.
- A set of new thermal assets will be operated according to the requirements and available data.
- The effect of events placed in the calendar will be taken into account.

CRediT authorship contribution statement

Joaquim Massana: Writing – review & editing, Writing – original draft, Visualization, Validation, Supervision, Methodology, Formal analysis, Data curation, Conceptualization. **Llorenç Burgas:** Writing – review & editing, Writing – original draft, Visualization, Validation, Supervision, Methodology, Investigation, Formal analysis, Data curation, Conceptualization. **Joan Colomer:** Writing – review & editing, Writing – original draft, Supervision, Conceptualization. **Andreas Sumper:** Writing – review & editing, Writing – original draft, Conceptualization. **Sergio Herraiz:** Writing – review & editing, Writing – original draft, Conceptualization.

Declaration of competing interest

The authors declare that they have no known competing financial interests or personal relationships that could have appeared to influence the work reported in this paper.

Data availability statement

The data associated with the study has not been deposited into a publicly available repository. Data will be made available on request by sending an e-mail to the authors.

Acknowledgements

This project was undertaken by the eXiT research group, recipient of the established research distinction (SITES group, Ref. 2021 SGR 01125) granted by the Generalitat de Catalunya.

The research received funding from the European Union Horizon 2020 under E-Land project grant agreement No 824388, from the European Union Horizon Europe under RESCHOOL project grant agreement No 101096490, and from MCIN/AEI/10.13039/501100011033 and the European Union NextGenerationEU/PRTR under OptiREC project grant agreement TED2021-131365B-C41.

The work of Andreas Sumper was supported by the Catalan Institution for Research and Advanced Studies (ICREA) Academia Program.

The authors extend their gratitude to Port of Borg, with special acknowledgement to Per Olav Dypvik and Dag Erik Eilertsen, for their valuable contributions to the data acquisition and results application sections.

References

[1] G. Maris, F. Flouros, The green deal, national energy and climate plans in Europe: member states' compliance and strategies, Adm. Sci. 11 (3) (2021) 75.
[2] W.M. Association, et al., State of the Global Climate 2021, 2022.
[3] J. Massana, L. Burgas, S. Herraiz, J. Colomer, C. Pous, Multi-vector energy management system including scheduling electrolyser, electric vehicle charging station and other assets in a real scenario, J. Clean. Prod. 380 (2022) 134996, https://doi.org/10.1016/j.jclepro.2022.134996.
[4] Y. Huang, W. Zhang, K. Yang, W. Hou, Y. Huang, An optimal scheduling method for multi-energy hub systems using game theory, Energies 12 (12) (2019) 2270.
[5] J. Liu, L. Ma, Q. Wang, Energy management method of integrated energy system based on collaborative optimization of distributed flexible resources, Energy 264 (2023) 125981, https://doi.org/10.1016/j.energy.2022.125981.
[6] Z. Mahmood, B. Cheng, N.A. Butt, G.U. Rehman, M. Zubair, A. Badshah, M. Aslam, Efficient scheduling of home energy management controller (hemc) using heuristic optimization techniques, Sustainability 15 (2) (2023), https://doi.org/10.3390/su15021378.
[7] M. Marzband, M. Ghadimi, A. Sumper, J.L. Domínguez-García, Experimental validation of a real-time energy management system using multi-period gravitational search algorithm for microgrids in islanded mode, Appl. Energy 128 (2014) 164–174, https://doi.org/10.1016/j.apenergy.2014.04.056.
[8] M. Motevasel, A.R. Seifi, Expert energy management of a micro-grid considering wind energy uncertainty, Energy Convers. Manag. 83 (2014) 58–72, https://doi.org/10.1016/j.enconman.2014.03.022.
[9] E. Sfikas, Y. Katsigiannis, P. Georgilakis, Simultaneous capacity optimization of distributed generation and storage in medium voltage microgrids, Int. J. Electr. Power Energy Syst. 67 (2015) 101–113, https://doi.org/10.1016/j.ijepes.2014.11.009.
[10] C.-S. Karavas, G. Kyriakarakos, K.G. Arvanitis, G. Papadakis, A multi-agent decentralized energy management system based on distributed intelligence for the design and control of autonomous polygeneration microgrids, Energy Convers. Manag. 103 (2015) 166–179, https://doi.org/10.1016/j.enconman.2015.06.021.
[11] G. Aghajani, H. Shayanfar, H. Shayeghi, Presenting a multi-objective generation scheduling model for pricing demand response rate in micro-grid energy management, Energy Convers. Manag. 106 (2015) 308–321, https://doi.org/10.1016/j.enconman.2015.08.059.
[12] W. Alharbi, K. Raahemifar, Probabilistic coordination of microgrid energy resources operation considering uncertainties, Electr. Power Syst. Res. 128 (2015) 1–10, https://doi.org/10.1016/j.epsr.2015.06.010.
[13] S. Talari, M. Yazdaninejad, M.-R. Haghifam, Stochastic-based scheduling of the microgrid operation including wind turbines, photovoltaic cells, energy storages and responsive loads, IET Gener. Transm. Distrib. 9 (12) (2015) 1498–1509, https://doi.org/10.1049/iet-gtd.2014.0040.
[14] C.L. Nge, I.U. Ranaweera, O.-M. Midtgård, L. Norum, A real-time energy management system for smart grid integrated photovoltaic generation with battery storage, Renew. Energy 130 (2019) 774–785, https://doi.org/10.1016/j.renene.2018.06.073.
[15] M.A. Ramli, H. Bouchekara, A.S. Alghamdi, Efficient energy management in a microgrid with intermittent renewable energy and storage sources, Sustainability 11 (14) (2019), https://doi.org/10.3390/su11143839.
[16] S. Sun, J. Fu, L. Wei, A. Li, Multi-objective optimal dispatching for a grid-connected micro-grid considering wind power forecasting probability, IEEE Access 8 (2020) 46981–46997, https://doi.org/10.1109/ACCESS.2020.2977921.
[17] F.A. Khan, K. Ullah, A. ur Rahman, S. Anwar, Energy optimization in smart urban buildings using bio-inspired ant colony optimization, Soft Comput. 27 (2) (2023) 973–989.
[18] A.U. Rehman, Z. Wadud, R.M. Elavarasan, G. Hafeez, I. Khan, Z. Shafiq, H.H. Alhelou, An optimal power usage scheduling in smart grid integrated with renewable energy sources for energy management, IEEE Access 9 (2021) 84619–84638.
[19] A. Alzahrani, K. Sajjad, G. Hafeez, S. Murawwat, S. Khan, F.A. Khan, Real-time energy optimization and scheduling of buildings integrated with renewable microgrid, Appl. Energy 335 (2023) 120640.

[20] D.S. Kumar, M. Premkumar, C. Kumar, S. Muyeen, Optimal scheduling algorithm for residential building distributed energy source systems using Levy flight and chaos-assisted artificial rabbits optimizer, Energy Rep. 9 (2023) 5721–5740.
[21] G. Volta, E.P. Jaeger, S. Vazquezmontiel, R. Hibbs, Introduction to evolutionary computing techniques, in: Proceedings Electronic Technology Directions to the Year 2000, IEEE Computer Society, Los Alamitos, CA, USA, 1995, pp. 122–127.
[22] J. Kennedy, R. Eberhart, Particle swarm optimization, in: Proceedings of ICNN'95 - International Conference on Neural Networks, vol. 4, 1995, pp. 1942–1948.
[23] W.D. Fisher, On grouping for maximum homogeneity, J. Am. Stat. Assoc. 53 (284) (1958) 789–798.
[24] S. Bhattacharya, P.K. Sadhu, D. Sarkar, Performance evaluation of building integrated photovoltaic system arrays (sp, tt, qt, and tct) to improve maximum power with low mismatch loss under partial shading, Microsyst. Technol. (2023).
[25] M. Cañigueral, J. Meléndez, Flexibility management of electric vehicles based on user profiles: the Arnhem case study, Int. J. Electr. Power Energy Syst. 133 (2021) 107195, https://doi.org/10.1016/j.ijepes.2021.107195.
[26] Central collection and publication of electricity generation, transportation and consumption data and information for the pan-European market, transparency.entsoe.eu, 2023.
[27] E. Aarts, J. Korst, W. Michiels, Simulated Annealing, Springer US, Boston, MA, 2005, pp. 187–210.
[28] R. Storn, K. Price, Differential evolution – a simple and efficient heuristic for global optimization over continuous spaces, J. Glob. Optim. 11 (1997) 341–359, https://doi.org/10.1023/A:1008202821328.
[29] An algorithm for least-squares estimation of nonlinear parameters, J. Soc. Ind. Appl. Math. 11 (2) (1963) 431–441, https://doi.org/10.1137/0111030.